THE JOURNAL OF COMPARATIVE NEUROLOGY 495:84–99 (2006)

Projections of the Nucleus Lentiformis Mesencephali in Pigeons (*Columba livia*): A Comparison of the Morphology and Distribution of Neurons with Different Efferent Projections

JANELLE M.P. PAKAN,[1] KIMBERLY KRUEGER,[2] ERIN KELCHER,[2]
SARAH COOPER,[3] KATHRYN G. TODD,[1,3,4] AND DOUGLAS R.W. WYLIE[1,2]*
[1]Centre for Neuroscience, University of Alberta, Edmonton, Alberta T6G 2E9, Canada
[2]Department of Psychology, University of Alberta, Edmonton, Alberta T6G 2E9, Canada
[3]Neurochemical Research Unit, University of Alberta, Edmonton, Alberta T6G 2E9, Canada
[4]Department of Psychiatry, University of Alberta, Edmonton, Alberta T6G 2E9, Canada

ABSTRACT

The avian nucleus lentiformis mesencephali (LM) is a visual structure involved in the optokinetic response. The LM consists of several morphologically distinct cell types. In the present study we sought to determine if different cell types had differential projections. Using retrograde tracers, we examined the morphology and distribution of LM neurons projecting to the vestibulocerebellum (VbC), inferior olive (IO), dorsal thalamus, nucleus of the basal optic root (nBOR), and midline mesencephalon. From injections into the latter two structures, small LM cells were labeled. More were localized to the lateral LM as opposed to medial LM. From injections into the dorsal thalamus, small neurons were found throughout LM. From injections into the VbC, large multipolar cells were found throughout LM. From injections into IO, a strip of medium-sized fusiform neurons along the border of the medial and lateral subnuclei was labeled. To investigate if neurons project to multiple targets we used fluorescent retrograde tracers. After injections into IO and VbC, double-labeled neurons were not observed in LM. Likewise, after injections into nBOR and IO, double-labeled neurons were not observed. Finally, we processed sections through LM for glutamic acid decarboxylase (GAD). Small neurons, mostly in the lateral LM, were labeled, suggesting that projections from LM to nBOR and midline mesencephalon are GABAergic. We conclude that two efferents of LM, VbC and IO, receive input from morphologically distinct neurons: large multipolar and medium-sized fusiform neurons, respectively. The dorsal thalamus, nBOR, and midline mesencephalon receive input from small neurons, some of which are likely GABAergic. J. Comp. Neurol. 495:84–99, 2006.

Indexing terms: optokinetic; optic flow; vestibulocerebellum; inferior olive, nucleus of the basal optic root; dorsal thalamus, GABA

Grant sponsor: Natural Sciences and Engineering Research Council of Canada (NSERC); Grant number: 170363 (to D.R.W.W.); Grant sponsor: Canadian Institute for Health Research; Grant number: 69013 (to D.R.W.W.); Grant number: 49622 (to K.G.T.); Grant sponsor: Davey Endowment for Brain Injury Research (to K.G.T.); Grant sponsor: NSERC (graduate fellowship to J.M.P.P.); Grant sponsor: Canada Research Chairs Program (to D.R.W.W.).

*Correspondence to: Douglas Wong-Wylie, Department of Psychology, University of Alberta, Edmonton, Alberta T6G 2E9, Canada. E-mail: dwylie@ualberta.ca

Received 26 May 2005; Revised 22 July 2005; Accepted 21 September 2005

DOI 10.1002/cne.20855

Published online in Wiley InterScience (www.interscience.wiley.com).

Self-motion through the environment results in patterns of "optic flow" across the entire retina (Gibson, 1954). Together, nuclei in the pretectum and the accessory optic system (AOS) are involved in the analysis of optic flow (Simpson, 1984; Simpson et al., 1988; Grasse and Cynader, 1990). The AOS and pretectum are highly conserved in vertebrates: the mammalian pretectal nucleus of the optic tract (NOT) is homologous to the nucleus lentiformis mesencephali (LM) in birds, and the avian nucleus of the basal optic root (nBOR) of the AOS is homologous to the medial and lateral terminal nuclei (MTN, LTN) of the mammalian AOS (Simpson, 1984; Fite, 1985; McKenna and Wallman, 1985a; Weber, 1985; Simpson et al., 1988).

Electrophysiological studies have shown that LM neurons have large receptive fields in the contralateral visual field and exhibit direction-selectivity to large-field moving visual stimuli (McKenna and Wallman, 1985b; Winterson and Brauth, 1985; Wylie and Frost, 1996; Wylie and Crowder, 2000). The LM receives primary input from the contralateral retina (Gamlin and Cohen, 1988a), and projects to several structures. These include ipsilateral projections to the medial column of the inferior olive (mcIO), nBOR, parts of the anterior dorsal thalamus, and structures along the midline in the mesencephalon. In addition, there is a bilateral mossy fiber projection to the vestibulocerebellum (VbC) that is primarily to folium IXcd (Clarke, 1977; Gamlin and Cohen, 1988b; Wild et al., 1989, 1998, 1999b; Wylie, 2001).

Studies have noted that the LM consists of several morphologically distinct types of neurons (Gottlieb and McKenna, 1986; Gamlin and Cohen, 1988b) with different immunochemical (Zayats et al., 2003) and intrinsic electrophysiological properties (Tang and Wang, 2002). However, it is not known if these different efferent projections originate from different neuronal subtypes. In the present study, using retrograde tracing techniques, we examined differences in the morphology and distribution of LM neurons that project to several different targets: the VbC, the mcIO, the nBOR, the dorsal thalamus, and structures along the midline of the mesencephalon.

MATERIALS AND METHODS

The methods reported herein conformed to the guidelines established by the Canadian Council on Animal Care and were approved by the Biosciences Animal Care and Policy Committee at the University of Alberta. Silver King and homing pigeons, obtained from various suppliers, were anesthetized with an intramuscular injection of a ketamine (65 mg/kg)/xylazine (8 mg/kg) cocktail and were given supplemental doses as needed to maintain anesthesia. The animals were placed in a stereotaxic device with pigeon ear bars and beak adapter so that the orientation of the skull conformed to the atlas of Karten and Hodos (1967). Sufficient skull and dura were removed to expose the brain surface and allow access to: the dorsal thalamus, the ventral tegmental area (VTA) and other midline structures, the VbC, the mcIO, or the nBOR. All target sites were localized using a stereotaxic atlas (Karten and Hodos, 1967). The dorsal thalamus and midline structures were identified exclusively through stereotaxic coordinates; however, for injections into the VbC, mcIO, and nBOR we also relied on single-unit recordings made with glass micropipettes (tip diameters 4–5 μm) filled with 2 M NaCl that were advanced using a hydraulic microdrive. Neurons in these structures respond to optic flow stimuli (e.g., Wylie and Frost, 1990; Winship and Wylie, 2001; Winship et al., 2005).

Studies using cholera toxin subunit B as a retrograde tracer

For injections into the VbC, mcIO, and nBOR, after recording from optic flow-sensitive cells, the recording electrode was replaced with a micropipette (tip diameter 20 μm) filled with Cholera Toxin Subunit B (CTB) (low-salt version, 104; List Biological Laboratories, Campbell, CA; 1% in 0.1 M phosphate-buffered saline [PBS, pH 7.4]) and the nucleus was located again by isolating cells responsive to large field visual stimuli. For all other target sites (dorsal thalamus and midline structures), injections were made according to the stereotaxic coordinates. In all cases the CTB was injected iontophoretically for 10–15 minutes (+4 μamps, 7 seconds on, 7 seconds off). Follow-

Abbreviations

AOS	accessory optic system
BC	brachium conjuctivum
CF	climbing fiber
CTB	cholera toxin subunit B
DAB	diaminobenzidine
dLGN	dorsal lateral geniculate nucleus
DLL	anterior dorsolateral thalamus, lateral subnucleus
FRM	mesencephalic reticular formation
GT	tectal gray
IO	inferior olive
LM, LMl, LMm	nucleus lentiformis mesencephali, pars lateralis, pars medialis
LPC	nucleus laminaris precommisuralis
LTN	lateral terminal nucleus
mcIO	medial column of the inferior olive
MpV	deep nucleus of the mesencephalon
MTN	medial terminal nucleus
nBOR	nucleus of the basal optic root
NOT	nucleus of the optic tract
nRT	nucleus rotundus
OKR	optokinetic response
PPC	nucleus principalis precommisuralis
Ru	red nucleus
SCE/I	stratum cellulare externum/internum
VbC	vestibulocerebellum
VTA	ventral tegmental area

Abbreviations Used in Figures

dl	dorsal lamella (of the inferior olive)
GLv	ventral leaflet of the lateral geniculate nucleus
LMv	lentiformis mesencephali, ventral region
MLF	medial longitudinal fasiculus
nIII	third cranial nerve (oculomotor nerve)
nXII	twelfth cranial verve (hypoglossal nerve)
nBORd	nucleus of the basal optic root, pars dorsalis
nBORp	nucleus of the basal optic root, proper
PV	nucleus posteroventralis thalami (Kuhlenbeck)
SOp	stratum opticum
TeO	optic tectum
TIO	tractus isthmo-opticus
TrO	tractus opticus
vl	ventral lamella (of the inferior olive)

ing the injection the micropipette was left in place for 5 minutes, then removed and the exposures were closed. Once the animal regained consciousness, buprenorphine (2 mg/kg, intramuscularly, i.m.) was administered as an analgesic.

After a survival time of 3–5 days postsurgery the animals were administered an overdose of sodium pentobarbital (100 mg/kg) and perfused with 0.9% saline followed by 4% paraformaldehyde in 0.1 M phosphate buffer (PB). The brain was extracted from the skull, embedded in gelatin, and placed in 30% sucrose in 0.1 M PB for cryoprotection. Using a microtome, frozen sections in the coronal plane (45 μm thick) were collected and sections were processed for CTB based on the protocol outlined by Wild (1993; see also Veenman et al., 1992). Sections were initially rinsed in 0.05 M PBS. They were then washed in a 25% methanol, 0.9% hydrogen peroxide solution for 30 minutes to decrease endogenous peroxidase activity. Sections were rinsed several times in PBS, then placed in 4% rabbit serum with 0.4% Triton X-100 in PBS for 30 minutes. Tissue was subsequently incubated for 20 hours in 0.005% polyclonal goat anti-CTB (product 703; lot 7032H; List Biological) with 0.4% Triton X-100 in PBS. Sections were then rinsed in PBS (several times) and incubated for 60 minutes in 0.16% biotinylated rabbit anti-goat antiserum (Vector Laboratories, Burlingame, CA) with 0.4% Triton X-100 in PBS. Tissue was rinsed several times with PBS and incubated for 90 minutes in 0.1% ExtrAvidin (Sigma, St. Louis, MO) with 0.4% Triton X-100 in PBS. Subsequent to a few washes with PBS the tissue was incubated for 12 minutes in filtered 0.025% diaminobenzidine (DAB) and 0.006% cobalt chloride in PBS. Then 0.005% hydrogen peroxide was added to the DAB solution and the sections were reacted for up to 6 minutes. The sections were then rinsed several times with PBS and mounted onto aluminum gelatin-coated slides, lightly counterstained with Neutral Red, and coverslipped with Permount.

Double-labeling fluorescent studies

We also performed double-labeling experiments using green and red fluorescent latex microspheres (Lumafluor, Naples, FL) as retrograde tracers. These were pressure-injected through a glass micropipette (tip diameter 20 μm) into the mcIO, VbC, and nBOR using a Picospritzer II (General Valve, Marietta, GA; 40 psi, 100 ms duration/puff). As with the CTB injections, these nuclei were first localized by recording the responses of neurons to optic flow stimuli. Following injection the electrode was undisturbed for 5 minutes. After a recovery period of 2–5 days the animals were deeply anesthetized with sodium pentobarbital (100 mg/kg) and immediately perfused with heparinized PBS (0.9% NaCl, 1 ml/100 ml heparin, 0.1 M phosphate buffer). The brains were extracted, then flash-frozen in 2-methylbutane and stored at −80°C until sectioned. Brains were embedded in optimal cutting temperature medium and 40-μm coronal sections were cut through the brainstem and cerebellum with a cryostat and mounted on electrostatic slides.

GAD immunohistochemistry

In a study of chicks, Zayats et al. (2003) showed that small LM neurons were GABAergic. In the present study, from injections into the nBOR, dorsal thalamus, VTA, and midline mesencephalon, small LM neurons were labeled (see Results). To have sufficient confidence in suggesting that these projections might involve GABAergic neurons, we felt it necessary to process sections through LM for GAD and perform a morphological analysis of GAD+ neurons.

The animals used for GAD immunochemistry were deeply anesthetized with sodium pentobarbital (100 mg/kg) and immediately perfused with 0.1 M PBS (0.9% NaCl) and 4% paraformaldehyde. The brains were extracted, embedded in optimal cutting temperature medium, and frozen. Coronal sections, 40 μm thick, were cut on a cryostat and mounted on electrostatic slides. After slides had dried completely, sections were rinsed with 0.1 M PBS and double-distilled water, washed with 0.15% H_2O_2 in 50% MeOH for 10 minutes to remove endogenous peroxidases, then rinsed in PBS and double-distilled water. Sections were blocked with 10% normal horse serum and 0.4% Triton X-100 in PBS for 1 hour at room temperature, then incubated in rabbit anti-GAD (65/67) polyclonal antibody (1:500; product AB1511; lot 25040055; Chemicon, Temecula, CA) in PBS for 24 hours at 4°C. The GAD 65/67 antibody is a synthetic peptide with the amino acid sequence [C]DFLIEEIERLGQDL from rat glutamate decarboxylase (GAD65; C-terminus residues [Cys] + 572-585; Erlander et al., 1991). The specificity of this polyclonal antibody, which was raised in rabbit, has been tested by several methods. Western blot analysis by the manufacturer reveals a doublet at ~65/68 kDa and immunocytochemistry experiments performed with this antibody have shown specificity in labeling GABAergic cell bodies and terminals in birds (pigeon: Theiss et al., 2003; owl: Rodriguez-Contreras et al., 2005). Immunohistochemical staining can be abolished by preincubation with 1–10 μg peptide per mL of diluted antibody. Sections were then rinsed with PBS and incubated in biotinylated goat anti-rabbit IgG (1:400; product Z0454; DakoCytomation, Mississauga, ON) with 0.4% Triton X-100 and 2.5% NHS in PBS for 2 hours. Control experiments with omission of the primary antibody revealed no specific labeling. After rinsing with PBS, sections were incubated with avidin biotin complex (1:100) for 30 minutes at room temperature. Immunoreactivity was then visualized using metal-enhanced 3,3′-diaminobenzadine tetrahydrochloride tablets (DAB; Sigma) for 1–5 minutes. Sections were rinsed with PBS and distilled water and dehydrated through graded ethanol and cleared in xylene before being coverslipped.

Microscopy

Sections were viewed with a compound light microscope (Leica DMRE) equipped with the appropriate fluorescence filters. The red and green latex microspheres fluoresce under rhodamine and FITC filters, respectively. The CTB- and GAD-reacted tissue was examined using standard light microscopy and drawings were made with the aid of a drawing tube. Images were obtained using an OPENLAB Imaging system (Improvision, Lexington, MA) and Adobe PhotoShop (San Jose, CA) software was used to compensate for brightness and contrast.

Morphological description and quantification of labeled neurons

Previous studies offered numerous descriptors for LM neurons including multipolar, stellate, ovoid, round, elliptical, piriform, spindle, and fusiform (Gottleib and McK-

enna, 1986; Gamlin and Cohen, 1988b; Wild, 1989; Tang and Wang, 2002; Zayats et al., 2003). When using CTB as a retrograde tracer there is very good labeling of the cell bodies and proximal dendrites, but labeling observed with Golgi or intracellular dyes is far more complete. For this reason, and to avoid excess subjectivity, we confined our morphological classification to fusiform, multipolar, or other. A fusiform neuron was elliptical in shape and tapering to two processes emerging from the poles of the cell body. A multipolar neuron had three or more processes emerging from the cell body. For quantitative measures, the length and width of the cell body were measured using images from OPENLAB and the area was calculated using the formula for an ellipse (length$\times$width$\times\pi/4$). A minimum of 50 cells were measured and morphologically classified for each projection area.

Nomenclature of LM

For the nomenclature of LM, we relied on Gamlin and Cohen (1988a,b), who divided the LM into medial and lateral subdivision (LMm, LMl). Both contain large and small cells (Gottleib and McKenna, 1986). Continuous with the LMl at its lateral and caudal aspects is the tectal gray (GT), which contains mainly small cells. The LMm, LMl, and the rostral part of GT all receive retinal input (Gamlin and Cohen, 1988a). The LMm is bordered medially by the nucleus laminaris precommissuralis (LPC), a thin strip of cells that does not receive input from the retina. Medial to LPC is the nucleus principalis precommissuralis (PPC), which is lateral to nucleus rotundus (nRt). In Nissl-stained sections the layers of the pretectum are relatively easy to distinguish, although the border between GT and LMl can be difficult to localize. Previously, the LMm was known as the LM magnocellularis (LMmc), and the LMl and GT were included as the LM parvocellularis (LMpc) (e.g., Karten and Hodos, 1967).

RESULTS

Experiments were performed on 23 pigeons. Eighteen pigeons were used for the retrograde studies using CTB. The injections of CTB into the nBOR (n = 3), VbC (n = 4), mcIO (n = 3), the dorsal thalamus (n = 4), and along the midline of the mesencephalon (n = 4), were all unilateral. Three birds were used for double-labeling fluorescence experiments. Two animals received injections of the fluorescent retrobeads in VbC and mcIO (cases VbC-IO #1 and 2) and the other pigeon received injections in nBOR and mcIO (case nBOR-IO). The remaining two animals were used for GAD-immunohistochemistry.

VBC-projecting LM neurons

Previous studies using anterograde techniques have shown that the LM projection to the VbC is a bilateral mossy fiber projection, which terminates in the granule layer as mossy fiber rosettes. This projection is primarily directed to folium IXcd but also includes folia VI-VIII (Clarke, 1977; Gamlin and Cohen, 1988b). We directed our injections to folium IXcd and first recorded the activity of Purkinje cells in response to optic flow stimuli. The complex spike activity of Purkinje cells (which is recorded in the molecular layer) in folium IXcd responds to patterns of optic flow resulting from either self-translation or self-rotation (Wylie and Frost, 1993, 1999a; Wylie et al., 1993, 1998). Once responsive neurons were found we moved the injection electrode into the adjacent granule cell layer.

From the injections into the VbC numerous neurons were observed in both LMl and LMm. In total, 69 LM cells were measured and morphologically classified. These neurons were large: length, 31.1 $\pm$ 1.0 μm (mean $\pm$ SEM, range 16–61 μm); width, 17.1 $\pm$ 0.5 μm (9–27 μm); area, 416.4 $\pm$ 17.3 μm^2 (149.9–769.7 μm^2). Usually the long axis of the cell was oriented dorsoventrally. Although a few of these neurons were fusiform, the vast majority were clearly multipolar (>85%). Figure 1A–C shows photomicrographs of neurons retrogradely labeled from the VbC.

Figure 3B shows a series of coronal sections through the LM illustrating the distribution of labeled cells from an injection in the VbC. The injection from this case, shown in the bottom row, included the granule cell layers at the base of folium IX, where IXab and IXcd are not completely separated. Labeled neurons were found throughout the rostrocaudal extent of LMm and LMl, but caudally most of the neurons were found ventrally and dorsally, rather than centrally.

mcIO-projecting LM neurons

The projection from the LM to inferior olive (IO) is restricted to the ipsilateral medial column (mcIO) (Clarke, 1977; Gamlin and Cohen, 1988b), which in turn projects as climbing fibers to the folia IXcd and X of the VbC (Arends and Voogd, 1989; Lau et al., 1998; Wylie et al., 1999b; Crowder et al., 2000). The LM projection to the mcIO is heavier to the caudal half (Wylie, 2001). Like the complex spike activity in the VbC, mcIO neurons can be identified based on their responses to optic flow patterns (Winship and Wylie, 2001).

Injections into the mcIO resulted in labeling of a relatively homogeneous population of neurons in LM. In total, 50 LM cells were measured and morphologically classified. These neurons were small to medium-sized (area, 223.7 $\pm$ 14.3 μm^2 [mean $\pm$ SEM], range 84.8–477.5 μm^2). They were somewhat shorter than most of the VbC-projecting LM neurons (length, 21.5 $\pm$ 0.64 μm, range 10–32 μm) and much thinner (width, 9.2 $\pm$ 0.3 μm, 6–18 μm). Invariably these neurons were fusiform with the long axis oriented dorsoventrally. Figure 1D–G shows photomicrographs of neurons retrogradely labeled from the mcIO.

Figure 3A shows a series of coronal sections through the LM illustrating the distribution of labeled cells from an injection in the mcIO. The majority of the cells were found in a densely packed dorsoventrally oriented strip along the border of LMm and LMl. Although difficult to determine conclusively, it appears that most of these cells were in LMm. Labeling was sparse in the rostral LM. The labeling from the mcIO injections appeared in areas devoid of labeling from the VbC injections. The complementary pattern of VbC and mcIO-projecting neurons can be seen by comparing the drawings in Figure 3A,B and the photomicrographs in Figure 1A,D.

nBOR-projecting LM neurons

The injections were positioned in nBOR based on the presence of cells responsive to largefield stimulation of the contralateral eye (Wylie and Frost, 1990). We have observed that the LM projection to the nBOR is heaviest to the dorsal region (unpubl. obs.). At least some of these fibers give collaterals to a region outside the nBOR, which we consider the lateral part of the VTA, and some fibers

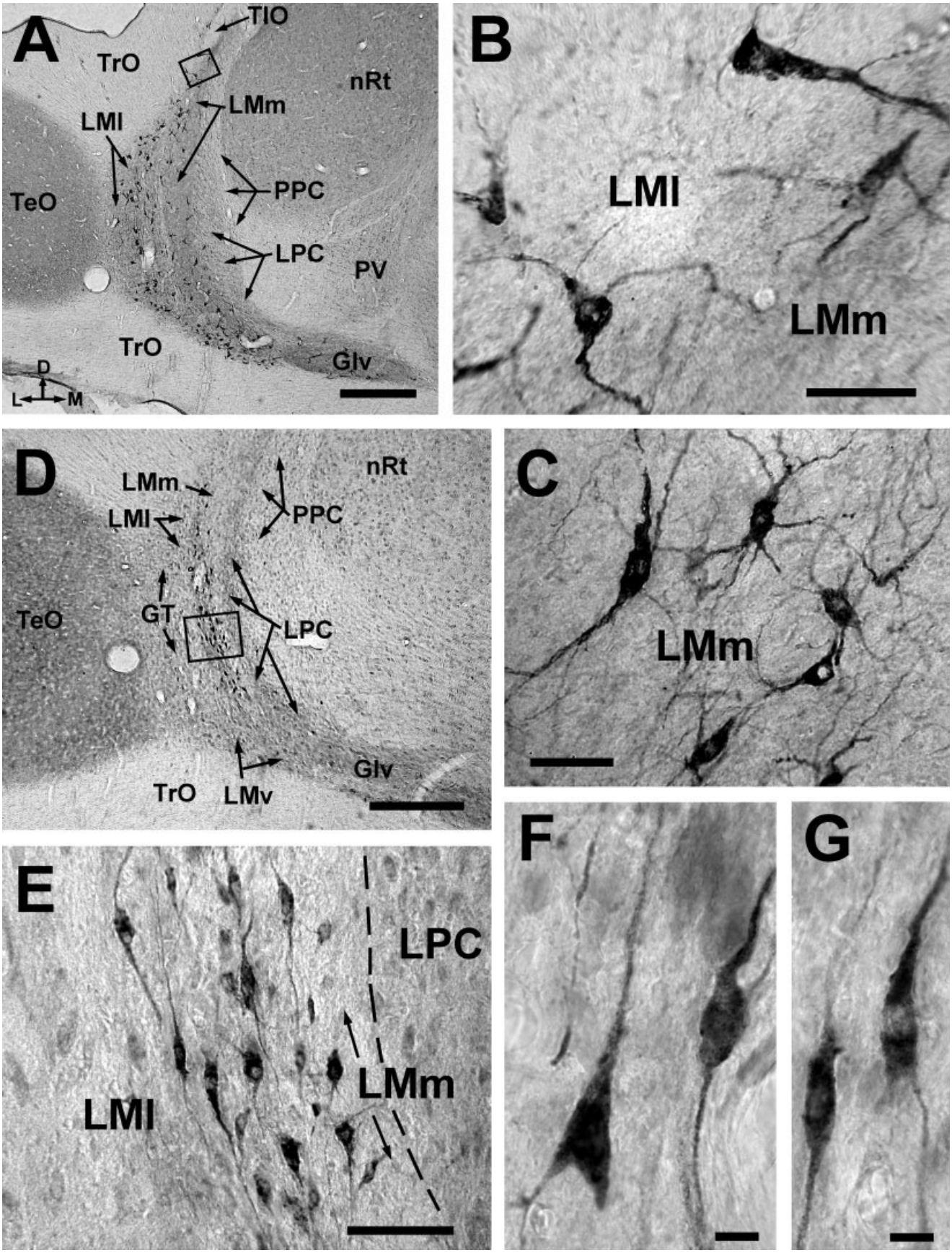

Fig. 1. Photomicrographs of coronal sections through the nucleus lentiformis mesencephali (LM) showing neurons labeled with cholera toxin subunit B. **A–C:** Cells labeled from injections in the vestibulocerebellum. In A, note the presence of labeled cells throughout the lateral and medial subnuclei of LM (LMl, LMm). The rectangle in A indicates the area shown in B. **D–G:** Cells labeled from an injection in the medial column of the inferior olive. In D and E, note the strip of tightly packed fusiform neurons on the LMm/LMl border. The rectangle in D indicates the area shown in E. For all panels, left is lateral (L), right is medial (M), and the top of the photomicrographs is dorsal (D). For additional abbreviations, see list. Scale bars = 500 μm in A,D; 50 μm in B,C,E; 10 μm in F,G.

continue into the accessory oculomotor region (Wylie et al., 1999a). In two of the cases the injections spread outside of the nBOR into the adjacent VTA, but the pattern of labeling was not different compared to the case in which the injection was confined to the nBOR.

Injections into the nBOR resulted in retrograde labeling of small LM neurons (length, 14.2 ± 0.26 μm, range 8–24 μm; width, 8.4 ± 0.16 μm, 5–14 μm; area, 93.2 ± 2.5 μm^2, 37.6–175.9 μm^2). In total, 119 LM cells were measured and morphologically classified. Most were classified as fusiform (67%) rather than multipolar (33%). As with the mcIO-projecting neurons, the long axis was usually oriented dorsoventrally. Figure 2A,B shows photomicrographs of neurons retrogradely labeled from the nBOR. Evident in Figure 2A, the majority of the nBOR-projecting neurons were found in LMl. This is emphasized in Figure 3C, which shows a series of coronal sections through the LM illustrating the distribution of labeled cells from an injection in the nBOR. Cells were found throughout the rostrocaudal extent of LM, with heavier labeling in the LMl as opposed to the LMm. Labeling was also extensive in the GT.

Dorsal thalamus-projecting LM neurons

Previous anterograde studies have shown that the projection from the pretectum to the anterior dorsolateral thalamus is primarily to the lateral subdivision (DLL), just dorsal to nRt (Wild, 1989; Wylie et al., 1998). In the four cases, stereotaxic injections were made into the thalamus and subsequent CTB processing of the injection site revealed that they were centered on the DLL. From these injections more cells were found in the tectum and GT compared to the LM. In total, 71 LM cells were measured and morphologically classified. The LM cells were small (length, 13.1 ± 0.31 μm, range 8–20 μm; width, 8.1 ± 0.21 μm, 4–12 μm; area, 83.7 ± 3.3 μm^2, 37.7–188.5 μm^2). As such, they resembled the nBOR-projecting LM neurons and fusiform and multipolar neurons were equally abundant. Figure 2C–F shows photomicrographs of retrogradely labeled thalamus-projecting LM neurons.

Figure 3D shows a series of coronal sections through the LM illustrating the distribution of labeled cells from an injection in the dorsal thalamus. The numerous cells found in the tectum were not drawn in the sections. Cells were found throughout the rostrocaudal extent of LM and were equally abundant in LMl and LMm. Note the extensive labeling in GT.

Midline mesencephalon injections: VTA/SCE-projecting neurons

Previous studies have also shown that the LM projects to structures along the midline in the mesencephalon; in particular, the ventral tegmental area (VTA), the stratum cellulare externum (SCE), the deep nucleus of the mesencephalon (MpV), the red nucleus (Ru), and the adjacent mesencephalic reticular formation (FRM; Gamlin and Cohen, 1988b; Wylie et al., 1999a). At least some axons originating in the LM that innervate the nBOR send collaterals to some of these other nuclei (Wylie et al., 1999a). In three cases we made injections along the midline in the mesencephalon. Because the injections involved multiple structures, these data should be interpreted with caution. In two cases the injections were quite large and extended a considerable distance along the midline. These injections were centered on the VTA and SCE, but also included the Ru, FRM, stratum cellulare internum (SCI), and other structures along the midline (e.g., the accessory oculomotor nuclei). In the third case the injection was smaller. It was centered on the red nucleus, but encroached upon adjacent structures including the VTA, SCE, and SCI, and possibly the accessory oculomotor nuclei along the midline. Nonetheless, the labeling in LM was similar for all three cases. In the pretectum there was very heavy labeling in the PPC and substantial labeling in the LPC. There was a moderate amount of labeling in LM, and generally the pattern of labeling resembled that from the nBOR injections: more cells were found in LMl compared to LMm and labeling was heavier ventrally. With respect to size and morphology, they also resembled the cells labeled from the nBOR and dorsal thalamus injections. In total, 131 LM cells were measured and morphologically classified. These LM cell were small (length, 13.8 ± 0.26 μm, range 8–24 μm; width, 8.3 ± 0.16 μm, 5–14 μm; area, 90.3 ± 2.63 μm^2, 26.0–221.1 μm^2) and most were fusiform (65%) as opposed to multipolar (35%).

Comparing the morphology and size of LM neurons

Figure 4 shows the silhouettes of LM neurons projecting to VbC, nBOR, dorsal thalamus, VTA/SCE, and mcIO, all drawn to the same scale. Clearly, the VbC neurons are much larger than the others and they tend to be multipolar rather than fusiform. The homogeneity of the mcIO-projecting LM neurons is represented in this figure: they were generally fusiform, oriented dorsoventrally and had a high aspect ratio (length:width). The cells projecting to the nBOR, dorsal thalamus, and VTA/SCE were all very similar. The only noticeable difference was that cells with a round profile were more prevalent among the thalamic- and VTA/SCE-projecting neurons.

GAD+ LM neurons

From the sections processed for GAD immunochemistry, neurons were labeled in the LM. The labeled cell bodies were rather pale in appearance, especially compared to labeling of GAD+ cells in other areas of the brain. For example, the labeling of cerebellar Purkinje cells and large neurons in the subpretectal nucleus and nucleus isthmi was much darker than those in LM. In total, 98 LM cells were measured and morphologically classified. The GAD+ LM cells were generally ovoid but processes were usually not apparent. The GAD+ cells were small (length, 12.5 ± 0.4 μm, range 8–20 μm; width, 8.3 ± 0.25 μm, 5–13 μm; area, 81.6 ± 3.46 μm^2, 37.6–163.4 μm^2) and similar in size to the nBOR-, thalamus-, and VTA/SCE-projecting neurons. The neuropil of LMm stained darker than that of LMl in these sections, but more GAD+ labeled cell bodies were apparent in LMl than LMm. Figure 3J,K shows GAD+ labeling in the LM.

Quantitative comparison of cell size

Figure 5 shows a plot of the distribution of the sizes (i.e., area in μm^2) of the different groups of neurons. The cells were grouped into 50-μm^2 bins and the relative percentage of cells falling into each bin is plotted by group. The distributions for the nBOR-, VTA/SCE-, thalamus-projecting, and GAD+ neurons were overlapping, thus indicating that the population(s) of neurons projecting to the nBOR, VTA/SCE, and thalamus cannot be distin-

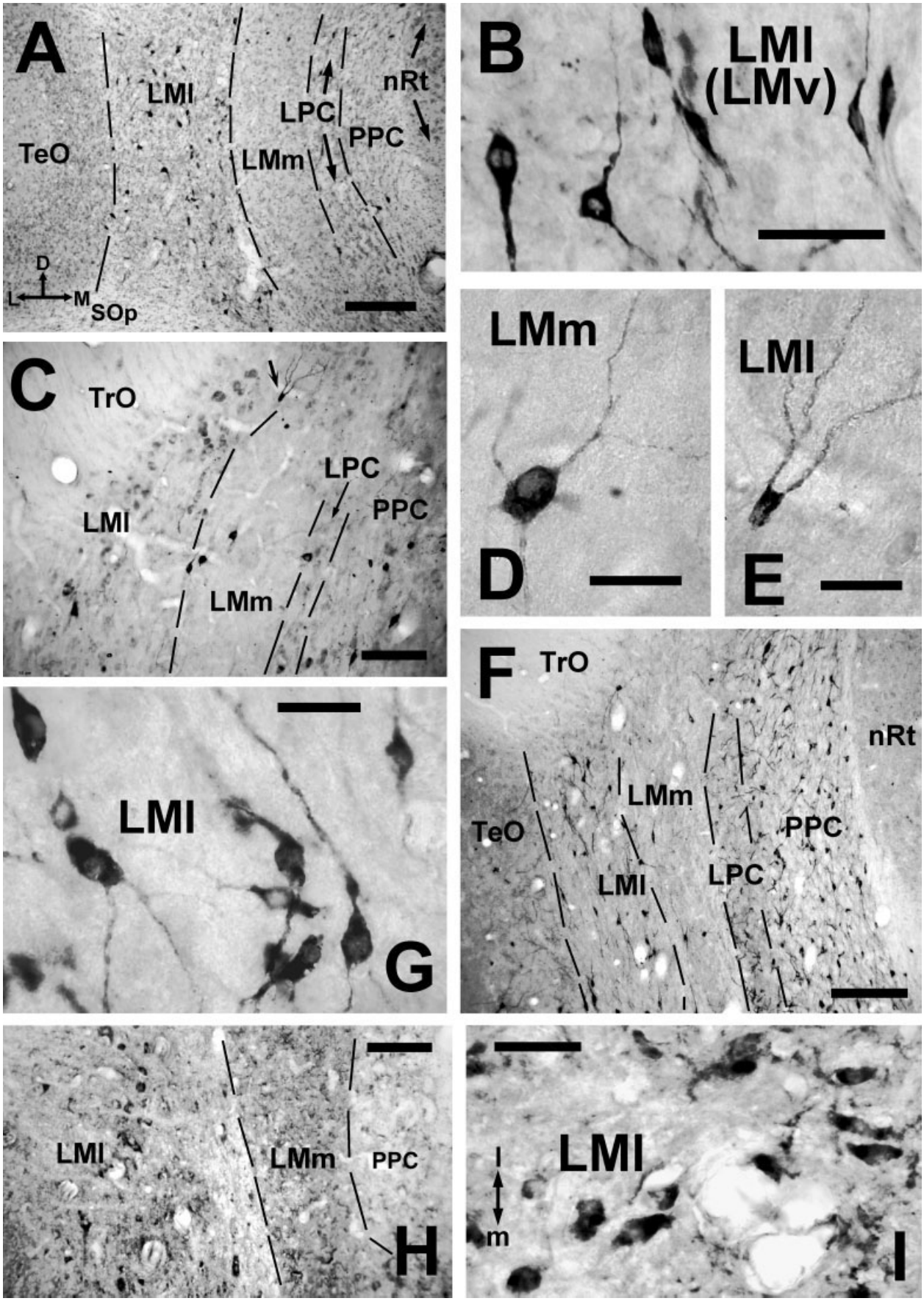
A
LMl
LPC
nRt
PPC
TeO
LMm
D
L
M
SOp
B
LMl
(LMv)
C
TrO
LPC
PPC
LMl
LMm
LMm
D
LMl
E
F
TrO
nRt
LMm
TeO
PPC
LMl
LPC
LMI
G
LMl
LMm
PPC
H
LMI
m
I

Figure 2

guished based on size, and that any of these projections may be GABAergic. The mcIO-projecting LM neurons formed a discrete distribution of medium-sized neurons. The VbC neurons show the greatest variability, but were clearly larger than the other three groups. To compare the different groups we performed a one-way analysis of variance (ANOVA) with six groups. There was a highly significant ($F(5,532) = 351.9$, $P = 0.00$) main effect of group. Post-hoc tests (Tukey HSD; α set to 0.05) revealed that the mcIO- and VbC-projecting neurons were significantly different from all other groups. The GAD+, nBOR-, thalamus-, and VTA/SCE-projecting LM neurons did not differ from each other.

Double-labeling fluorescent studies

In two birds different colors of fluorescent microspheres were injected into the VbC and IO. In total there were 348 LM neurons labeled from the VbC injections and 366 LM neurons labeled from the mcIO injections. No neurons were double-labeled, indicating that LM cells projecting to VbC do not send collateral branches to IO. Figure 6A,B shows photomicrographs from case VbC-IO#1 in which the red tracer was injected into the VbC and green was injected into the mcIO. Note the larger size of the VbC-projecting neurons. Figure 6C shows data from case VbC-IO#2 in which the red and green tracers were injected into the mcIO and VbC, respectively. The typical pattern of mcIO labeling in the caudal region of the LM (red cells) is apparent: a strip of tightly packed neurons running dorsoventrally. There was only a single VbC-projecting neuron in the vicinity of this group.

In case nBOR-IO, the red tracer was injected into the mcIO and the green tracer was injected into the ipsilateral nBOR. The nBOR injection spread quite a bit dorsally, but the average size of the retrogradely labeled cells (15.0×8.0 μm) was close to that of the LM cells labeled from the CTB injections in the nBOR. There were 424 and 140 LM neurons labeled from the nBOR and IO injections, respectively. There were no double-labeled neurons, indicating that LM cells projecting to nBOR do not send collaterals to the IO. Figure 6D shows photomicrographs from case nBOR-IO.

DISCUSSION

Previous electrophysiological studies have shown that LM neurons exhibit direction-selectively to largefield stimuli moving in the contralateral visual field (Winterson and Brauth, 1985; Wylie and Frost, 1996; Wylie and Crowder, 2000). The LM has been linked to the analysis of optic flow in general, and the generation of the optokinetic response (OKR) in particular (for review, see Simpson et al., 1988; birds: McKenna and Wallman, 1981, 1985b; Gioanni et al., 1983). Neuroanatomical studies emphasize that LM is not homogeneous, but consists of several different cell types (Gottlieb and McKenna, 1986; Zayats et al., 2003). In the present study we have shown that morphologically distinct LM neurons project to different structures (Fig. 7). From injections into the VbC, large multipolar neurons were labeled throughout most of LMl and LMm, with the exception of a region on the border of LMm and LMl. In this region, medium-sized fusiform neurons were labeled after injections into the mcIO. The double-labeling studies involving paired injections into the VbC and mcIO further emphasized that these projections arose from completely separate populations. Gamlin and Cohen (1988b) also noted these morphological and distributional differences between VbC- and mcIO-projecting LM neurons. They examined the VbC projection with injection of retrograde tracer into the brachium conjuctivum (BC). They described the retrogradely labeled LM neurons as multipolar but of a slightly smaller size (20–24 μm) than that reported in the present study. Their injections in BC also labeled numerous cells in LPC that were not observed with the injections into the cerebellum in the present study. Perhaps the LPC labeling observed by Gamlin and Cohen (1988b) resulted from spread of the BC into the lateral pontine nucleus, which does receive a substantial projection from LPC (Gamlin and Cohen, 1988b).

From injections into the VTA/SCE, nBOR and dorsal thalamus, small neurons were labeled in the LM. From the injections into the dorsal thalamus, small fusiform and multipolar neurons were labeled in LMm and LMl. This projection has been previously described by Wild (1989) and Wylie et al. (1998), but no details with regard to soma size were provided in those studies. From the injections into nBOR and VTA/SCE, we observed small neurons primarily in LMl. The projection from the LM to nBOR was first described by Azevedo et al. (1983), but soma size was not reported. Compared to the dorsal thalamic-projecting neurons, relatively more of the nBOR- and VTA/SCE-projecting neurons were fusiform. Although there is some overlap with respect to the sizes of the mcIO-projecting neurons and the small LM neurons, a double-labeling experiment revealed that the nBOR- and mcIO-projecting neurons arise from completely separate populations. It is certain that at least some of the LM neurons projecting to the nBOR also project to VTA/SCE. Wylie et al. (1999a) traced individual axons of LM neurons labeled with biotinylated dextran amine. They found that some axons terminating in the VTA also provided collaterals to nBOR. Unfortunately, the proximity of the nBOR to the VTA/SCE, and the fact that axons of neurons to the SCE and VTA pass just dorsal to nBOR, made a double-labeling experiment next to impossible. We did, however, observe varicosities indicative of terminal labeling in the dorsomedial margin of nBOR from injections of CTB into VTA/SCE. This terminal labeling was rather heavy and was found among heavy retrograde labeling in this part of nBOR, thus reconstruction of these axons would be impractical. Given the results of the anterograde study by Wylie et al. (1999a), we believe that these terminals in the

Fig. 2. Small neurons in the nucleus lentiformis mesencephali (LM). Photomicrographs of coronal sections through LM, showing retrogradely labeled neurons from injections of cholera toxin subunit B into the nucleus of the basal optic root (nBOR) (**A,B**), dorsal thalamus (**C–F**), and the midline mesencephalon (ventral tegmental area, stratum cellulare externum, VTA/SCE) (**G–I**). Most of the nBOR- and VTA/SCE-projecting LM neurons were fusiform (B,H,I) and more were found in the LMl compared to the LMm (A,G). From the injections into the VTA/SCE, more labeling was found in the nucleus principalis precomissuralis (PPC) compared to the LM (G). From the injections into the dorsal thalamus, neurons were found in both LMl and LMm (C–E), but more neurons were found in the tectal gray (not shown). The arrow in C indicates the labeled cell shown in E. Left is lateral (L) and right is medial (M) for all panels except I and the top of the photomicrographs is dorsal (D). For additional abbreviations, see list. Scale bars = 200 μm in A,G; 100 μm in C,J; 50 μm in B,F; 25 μm in D,E,H,I.

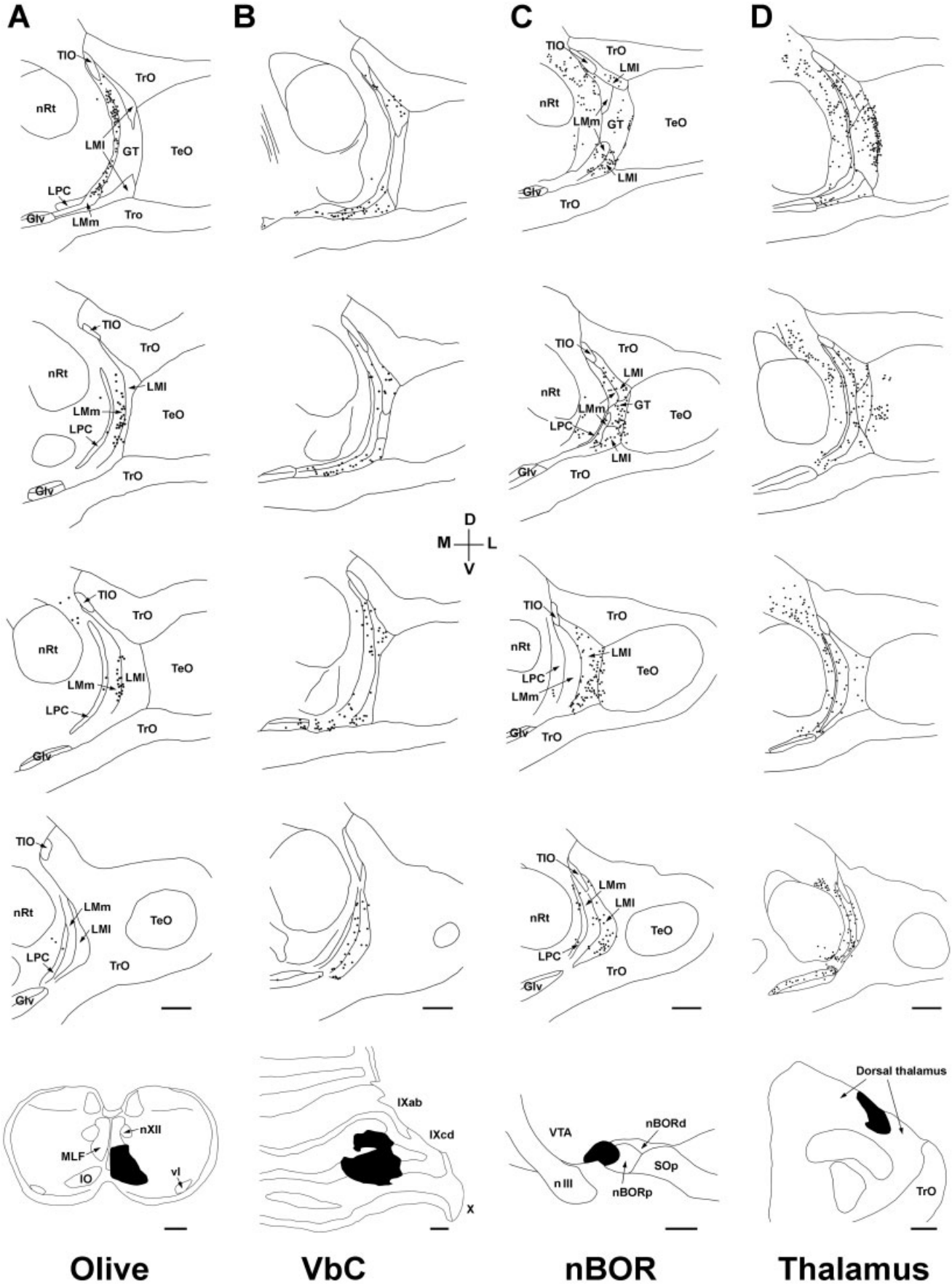
A
B
C
D
TIO
TrO
nRt
LMl
GT
TeO
LPC
Glv
LMm
Tro
D
M
L
V
nXII
MLF
IO
vl
IXab
IXcd
x
VTA
nBORd
SOp
n III
nBORp
Dorsal thalamus
Olive
VbC
nBOR
Thalamus

Figure 3

dorsomedial nBOR arose from collaterals of VTA/SCE-projecting axons originating in LM.

There were some projections of LM that were not investigated in the present study. These include a projection to the PPC and nuclei in the ventral pons. It has been reported that this latter projection originates mainly in LPC (Gamlin and Cohen, 1988b).

Comparisons with previous anatomical studies

Using Golgi-staining as well as light and electron microscopy, Zayats et al. (2003) described several cell types in the LMmc (i.e., LMl) of chicks. Large- (50–65 × 25–32 μm [length × width]) and medium-large (32–35 × 18–20 μm) cells were described as multiangular. Medium-sized neurons were described as multiangular (25–26 μm long) or elongated (20–24 μm long), and small neurons (13–17 μm long) were described as round or ovoid. The medium, medium-large, and large multiangular neurons correspond well with the multipolar VbC-projecting neurons described in the present study. Likewise, the medium elongated cells described by Zayats et al. (2003) correspond with the medium-sized fusiform neurons projecting to the mcIO, and the small ovoid/round neurons correspond with the nBOR-, VTA/SCE-, and thalamus-projecting neurons described in the present study.

Zayats et al. (2003) determined that the small neurons in the chick LMmc were GABAergic, insofar as they exhibited GAD-immunoreactivity. Granda and Crossland (1989) and Domenici et al. (1988) also noted that GABAergic cells in the avian LM are small, and this has also been noted in other species (e.g., frogs, Li and Fite, 1998). Zayats et al. (2003) suggested that the GABAergic LM neurons were interneurons, but the data from the present study suggest that these GABAergic LM neurons may project to the nBOR, VTA/SCE, and dorsal thalamus. We found that the GAD+ LM neurons were small and indistinguishable in size from the nBOR-, VTA/SEC-, and dorsal thalamus-projecting neurons in LM. We also found that GAD+ neurons were more prevalent in LMl than LMm, much like the distribution of nBOR- and VTA/SCE-projecting neurons. This strongly suggests that some of the nBOR- and VTA/SCE-projecting neurons are GABAergic.

Fig. 3. Distribution of retrograde labeling in the pretectum from various injections of cholera toxin subunit B. Four coronal sections, at 180-μm intervals, through the pretectum are shown from caudal (top) to rostral. The injection sites are shown in the bottom row. From injections into the medial column of the inferior olive (mcIO, **A**), the majority of the cells were found in a densely packed dorsoventrally oriented strip along the border of LMm and LMl. From injections into the vestibulocerebellum (VbC, **B**), labeled neurons were found throughout the rostrocaudal extent of LMm and LMl, but caudally, along the border of LMm and LMl, the central region where labeling from mcIO injections was observed was void of labeled cells from VbC injections. The complementary pattern of VbC and mcIO projecting neurons can be seen by comparing A and B. From injections into the nucleus of the basal optic root (nBOR, **C**), labeled cells were found throughout the rostrocaudal extent of LM, with heavier labeling in the LMl compared to the LMm. From injections into the dorsal thalamus (**D**), labeled cells were found throughout the rostrocaudal extent of LMl and LMm, with extensive labeling in GT. Lateral (L), medial (M), dorsal (D), ventral (V). For more abbreviations, see list. Scale bars = 200 μm (applies to all).

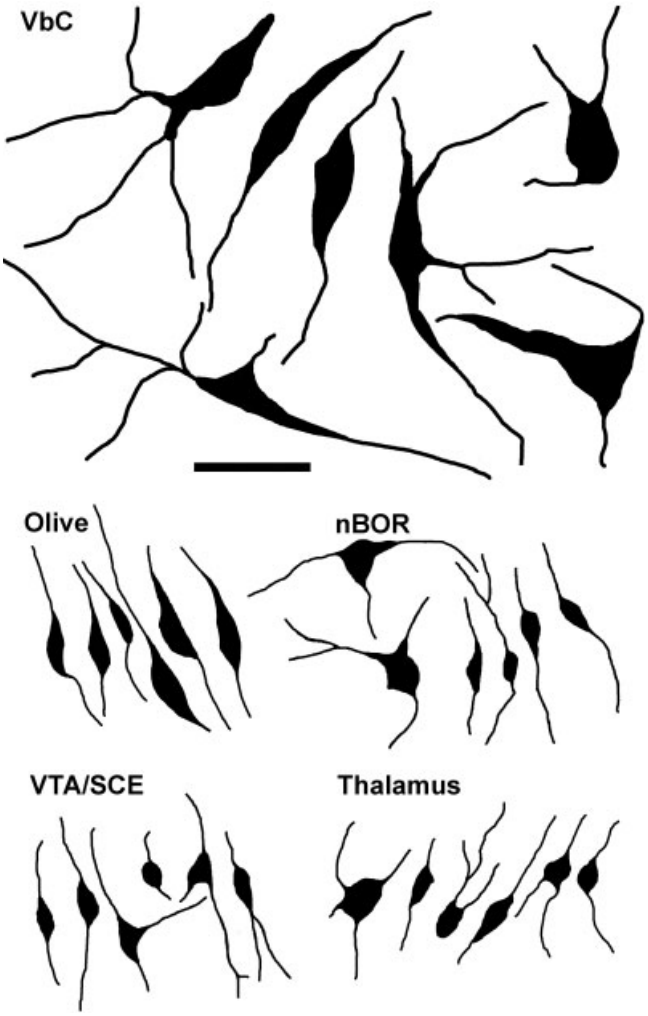

Fig. 4. A comparison of the morphology of neurons in the nucleus lentiformis mesencephali (LM) that project to the vestibulocerebellum (VbC), the medial column of the inferior olive, the ventral tegmental area/stratum cellulare externum (VTA/SCE), the nucleus of the basal optic root (nBOR), and the dorsal thalamus. The VbC neurons are much larger than the others and they tend to be multipolar rather than fusiform. The mcIO-projecting LM neurons were generally fusiform, oriented dorsoventrally with a high aspect ratio (length:width). The cells projecting to the nBOR, dorsal thalamus, and VTA/SCE were similar, but cells with a round profile were more prevalent among the thalamic- and VTA/SCE-projecting neurons. Scale bar = 50 μm (applies to all).

Proposed functions of the different types of LM neurons

Previous recording studies have characterized LM neurons as having very large receptive fields, responsive to moving largefield stimuli (McKenna and Wallman, 1985b; Winterson and Brauth, 1985; Wylie and Frost, 1996; Wylie and Crowder, 2000). The results of the present study, along with previous studies (e.g., Zayats et al., 2003; Tang and Wang, 2002), emphasize that the LM should not be regarded as a homogeneous structure, but rather consists of morphologically distinct subtypes of neurons with particular projections. Furthermore, al-

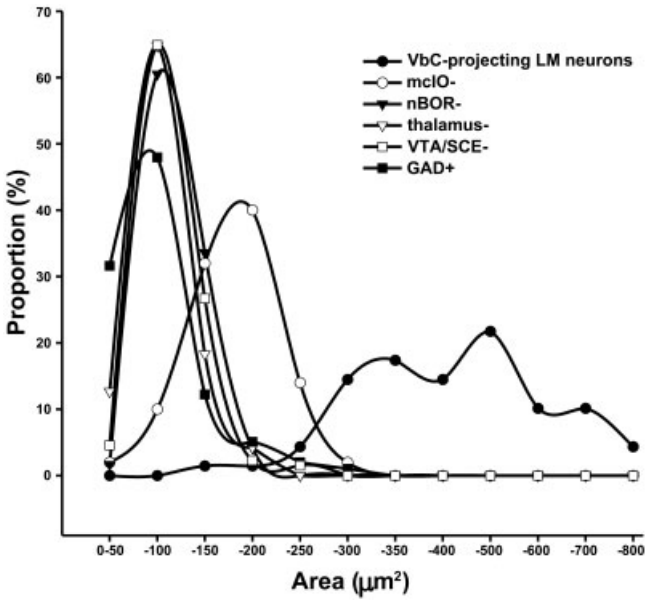

Fig. 5. Distribution of the sizes of neurons in the nucleus lentiformis mesencephali (LM). Under the assumption that the cross-section of the neurons could be approximated by an ellipse, the sizes (μm^2) of neurons were calculated and then grouped into 50-μm bins. The relative percentage of cells falling into each bin is plotted by group. LM neurons retrogradely labeled from the vestibulocerebellum (VbC), medial column of the inferior olive (mcIO), nucleus of the basal optic root (nBOR), the ventral tegmental area/stratum cellulare externum (VTA/SCE), and the dorsal thalamus are represented by the indicated symbols, as are GAD+ LM neurons. The distributions for the nBOR-, VTA/SCE-, thalamus-projecting, and GAD+ neurons were overlapping. Statistical analysis revealed that the mcIO-projecting LM neurons formed a discrete distribution of medium-sized neurons. The VbC neurons show the greatest variability, but were clearly larger than the other three groups. The mcIO- and VbC-projecting neurons were significantly different from all other groups. The GAD+, nBOR-, thalamus-, and VTA/SCE-projecting LM neurons did not differ from each other.

though risking an overstatement, we would argue that the present study speaks to a bias in the neurophysiological literature. In both birds and mammals the majority of the electrophysiological research has examined the pretectal pathways to the parts of the inferior olive that provide climbing fiber (CF) input to the VbC (see below). Clearly, this olivo-VbC pathway originates from a single cell type and from an isolated area in LM. Much less is known about pathways that originate from different types of pretectal neurons. A critical line of inquiry in this regard is, do the various types of pretectal neurons differ with respect to physiological properties and/or mediate different behaviors? Few studies address this issue and many more studies are needed to understand the various roles of the different cell types in visual information processing. Nonetheless, as illustrated in Figure 7 and discussed below, we offer an attempt at ascribing different roles to the different types of LM neurons.

Function of the medium-sized fusiform LM neurons projecting to the inferior olive

The olivo-cerebellar pathway projecting to the VbC and originating in the pretectum has been studied in detail in numerous species (see Simpson et al., 1988). The complex spike activity (CSA) of Purkinje cells (which reflects CF input; Eccles et al., 1966) responds best to particular patterns of optic flow resulting from either self-translation or self-rotation (birds: Wylie and Frost, 1991, 1993, 1999a; Wylie et al., 1993, 1998, 1999b; Winship and Wylie, 2001; mammals: Simpson et al., 1981; Graf et al., 1988; Leonard et al., 1988; van der Steen et al., 1994), and these neurons are critical for mediating the OKR (e.g., Robinson, 1976; Zee et al., 1981; Ito et al., 1982; Nagao, 1983; Waespe et al., 1983; Lisberger et al., 1984). Those neurons responsive to translational optic flow have been linked to head-bobbing (Wylie et al., 1993; Wylie and Frost, 1999b), an OKR that is stereotypical in pigeons and some other birds (Friedman, 1975; Frost, 1978).

A further clarification of the role of the pretectal olivo-VbC pathway can be gleaned from a line of inquiry initiated by Ibbotson et al. (1994). They recorded the responses of neurons in the wallaby NOT in response to drifting sine wave gratings of varying spatial and temporal frequency (SF, TF). They found that pretectal neurons could be classified into two groups: those that preferred low SF/high TF gratings vs. those that preferred high SF/low TF stimuli. As speed = TF/SF, Ibbotson et al. (1994) referred to these two groups as *fast* and *slow* pretectal neurons. Subsequently, Wylie and Crowder (2000) found that pigeon LM neurons also fall into fast and slow groups based on spatiotemporal tuning. The concordance between the pigeon LM and wallaby NOT in this respect is remarkable (Ibbotson and Price, 2001). In the pigeon LM, the fast cells outnumber the slow cells by 2:1. Winship et al. (2005) recorded the CSA in the pigeon VbC and found that they responded best to slow gratings. Thus, the medium-sized fusiform LM neurons are slow neurons. Ibbotson et al. (1994) suggested that the slow neurons were important for the maintenance of the OKR when retinal slip velocities are low. As such, the slow neurons are more responsive during the indirect as opposed to the direct OKN, and involved in charging the velocity storage at lower retinal slip speeds.

Function of the large multipolar LM neurons projecting to the VbC

The LM-VbC mossy fiber projection is quite unique and a homologous NOT-VbC pathway has not been described in mammals. In the present study we show that it arises from the large multipolar neurons in LM. The nBOR also provides a direct mossy fiber pathway to the VbC in pigeons (Brecha et al., 1980; Wylie et al., 1997), and it appears that most of these cells are medium to large multipolar neurons (Brecha et al., 1980). In turtles an nBOR-cerebellar pathway has also been reported, and this arises from medium and large neurons, but not small neurons (Reiner and Karten, 1978). In fish, mossy fiber pathways to the cerebellum, originating in the homologs of nBOR and LM, have also been described (Finger and Karten, 1978). However, these pathways have not been described in frogs (Montgomery et al., 1981). Finally, projections from the lateral and medial terminal nuclei (LTN, MTN) of the AOS have been found in some mammalian species (chinchilla: Winfield et al., 1978; tree shrew: Haines and Sowa, 1985) but not others (cats: Kawasaki and Sato, 1980; rats and rabbits: Giolli et al., 1984).

There are little data as to the function of the pretectal-VbC and AOS-VbC pathways and how they might differ

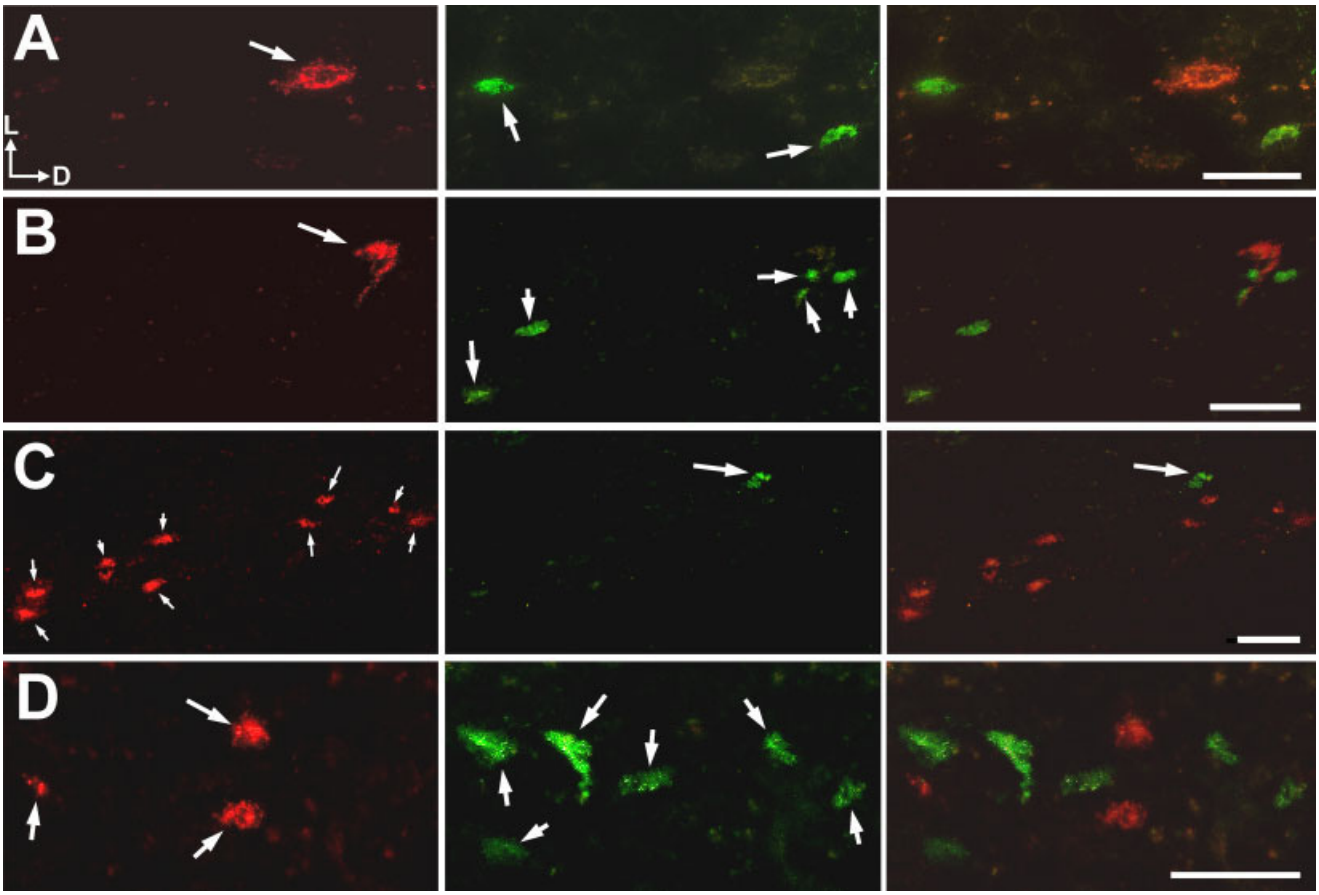

Fig. 6. Photomicrographs of coronal sections through the nucleus lentiformis mesencephali (LM) showing cells labeled with fluorescent microspheres. In **A–E**, triptychs are shown: the left and middle panels show the section viewed with the rhodamine and FITC filters, respectively, and the right panels show the overlay. A and B show data from case VbC-IO#1 in which the red microspheres were injected into the vestibulocerebellum (VbC) and the green microspheres were injected into the medial column of the inferior olive (mcIO). Note the larger size of the VbC-projecting neurons. C shows data from case VbC-IO#2 in which the green and red microspheres were injected into the VbC and mcIO, respectively. The typical pattern of mcIO labeling in the caudal region of the LM (red cells) is apparent: a strip of tightly packed neurons running dorsoventrally. There was only a single VbC-projecting neuron in the vicinity of this group. D shows data from case IO-nBOR in which the green and red microspheres were injected into the nBOR and mcIO, respectively. There were no double-labeled neurons in any of the cases. For all panels, right is dorsal (D) and the top of the photomicrographs is lateral (L). The arrows indicate labeled neurons. Scale bars = 50 μm (applies to all).

from other efferent pathways of the AOS and pretectum. Winship et al. (2005) recorded the responses of mossy fiber rosettes in the VbC to largefield drifting gratings. As these units were located in the VbC and responsive to largefield stimuli, Winship et al. (2005) assumed that these units were from the endings of mossy fibers that originated in the LM and nBOR. From this sample, units preferring slow or fast gratings were equally abundant. Thus, with respect to spatial-temporal tuning, whereas the medium-sized fusiform LM neurons are slow neurons (see above), the large multipolar neurons are either fast or slow neurons. Following the arguments of Ibbotson et al. (1994) with respect to the role of fast vs. slow pretectal neurons, both the medium-sized fusiform LM neurons projecting to the mcIO and the large multipolar VbC-projecting LM neurons are involved in processing slow speeds for charging the velocity storage mechanism when retinal slip velocities are low. The large multipolar neurons responding to fast stimuli would be involved when retinal slip velocities are high, such as the latent period at the onset of optokinetic stimulation ("open loop OKR").

Functions of the small LM neurons projecting to the nBOR

In the present study we found that small LM neurons project to the nBOR, and we suggested that these may be GABAergic. Electrophysiological studies lend support to the assertion that the nBOR-projecting LM neurons are, at least in part, GABAergic. In turtles, Ariel and Kogo (2005) noted that the nBOR receives an inhibitory input ("shunting inhibition") from LM, which is blocked by a $GABA_A$ receptor antagonist. Nogueira and Britto (1991) recorded from nBOR neurons in pigeons in response to electrical stimulation of LM. This projection is directed generally toward nBOR neurons that prefer horizontal motion. Most of the neurons preferring temporal-to-nasal motion were excited in response to LM stimulation, but most of those preferring nasal-to-temporal motion were

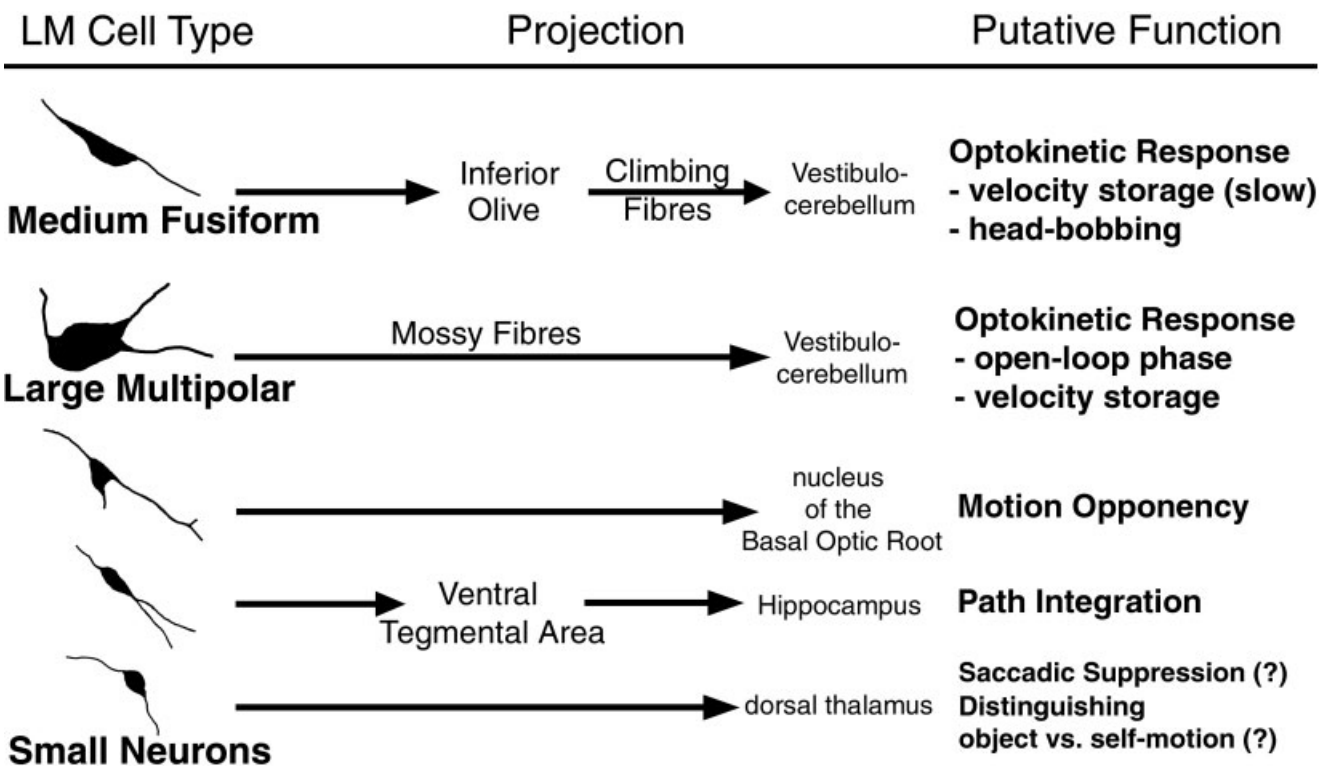

Fig. 7. A summary of the projections of neurons in the nucleus lentiformis mesencephali. The projections of the large multipolar, medium-sized fusiform, and small neurons are shown, along with their associated putative functions, as discussed in the text.

inhibited. Thus, perhaps these latter units are receiving a disproportionate input from GABAergic LM neurons. The GABAergic projection from LM to nBOR may represent a critical step in creating fully motion opponent responses in nBOR. Like LM neurons, nBOR neurons exhibit direction-selectivity to largefield stimuli moving in the contralateral visual field (Burns and Wallman, 1981; Morgan and Frost, 1981; Wylie and Frost, 1990). Most nBOR neurons are fully motion opponent in that they exhibit excitation to motion in one (preferred) direction and are inhibited by motion in the opposite (antipreferred) direction. In the basic delay-and-compare motion detector, which has been used to model NOT, LM, and nBOR neurons (Ibbotson et al., 1994; Wolf-Oberhollenzer and Kirshfeld, 1994; Crowder et al., 2003), motion opponency is established by the "subtraction" or "balance" step. This step of the model involves pooling the responses of two half-detectors with opposite direction preferences. If the output of one of the half-detectors is inhibitory, the result is a fully motion opponent response (e.g., Ibbotson et al., 1994; Ibbotson and Clifford, 2001; Zanker et al., 1999). Perhaps the small GABAergic LM neurons represent the half-detectors with the inhibitory outputs for the fully motion opponent nBOR neurons.

Functions of the small LM neurons projecting to the dorsal thalamus

In the present study we showed that small neurons distributed throughout LMm and LMl project to the dorsal thalamus. A pretecto-thalamic pathway has been demonstrated in numerous species. In mammals it has been shown that this projection is directed to the dorsal lateral geniculate nucleus (dLGN) and originated mainly in NOT (e.g., Graybiel and Berson, 1980; Bickford et al., 2000; see also Simpson et al., 1988). In reptiles it has also been shown that the LM projects to the dLGN (Kenigfest et al., 2000). In birds the equivalent of the LGN are the retinal-recipient nuclei of the anterior dorsal thalamus, which includes DLL (Karten et al., 1973; Karten and Shimizu, 1989). In turtles, cats, and monkeys it has been demonstrated that the pretectal-dLGN projection is largely GABAergic (Cucchiaro et al., 1991; Wahle et al., 1994; Kenigfest et al., 2004; for review, see van der Want et al., 1992). Kenigfest et al. (2004) speculated that the equivalent projection in pigeons is also likely GABAergic, and data from the present study do lend support, insofar as small LM neurons projected to the dorsal thalamus, and GAD+ LM neurons were small.

Little is known about the function of the pretectal to dorsal thalamus projection, but there are two possibilities. First, this projection could mediate saccadic suppression. During a saccade it has been demonstrated that neurons in the dorsal thalamus pause, presumably so that the retinal motion occurring during the saccade is not processed by the thalamofugal system (e.g., Zhu and Lo, 1996). It is known that GABAergic inhibition originating in the superior colliculus mediates the pause (Zhu and Lo, 1996), but it is possible that pretectal GABAergic neurons have a similar function. Second, Wylie et al. (1998) suggested that this projection may somehow be involved in

distinguishing object-motion from self-motion. Frost (1985) emphasized that, whereas the pretectum and AOS process optic flow resulting from self-motion, the thalamofugal and tectofugal systems process local motion, which results from objects moving in the environment. Optic flow is generally interpreted as due to self-motion and is not confused with object-motion. Perhaps the pretectal to dorsal thalamus projection is important in this process.

Functions of the small LM neurons projecting to the VTA

In the present study we showed that small neurons, most of which localize to LMl, project to the VTA. Both nBOR and LM project to the VTA, which in turn projects to the hippocampus (Casini et al., 1986). Wylie et al. (1999a) suggested that the VTA-hippocampus projection might be important for conveying optic flow information for "path integration," a form of spatial navigation whereby an animal can determine spatial relationships such as the origin and destination of motion based on ideothetic cues from self-motion. The hippocampus is critical for this behavior (Foster et al., 1989; Wilson and McNaughton, 1993; McNaughton et al., 1995, 1996; Whishaw et al., 1997; Whishaw and Maaswinkel, 1998). Original studies suggested that ideothetic information for self-motion comes from the vestibular system (McNaughton et al., 1995, 1996; Muller et al., 1996) but Wylie et al. (1999a) proposed optic flow as an additional ideothetic cue. This assertion is supported by the fact that both vestibular and visual motion cues influence some place cells in the hippocampus and may thus be used for path integration (Sharp et al., 1995).

In summary, we found that two efferents of LM, VbC and IO, receive input from morphologically distinct neurons: large multipolar and medium-sized fusiform neurons, respectively. The dorsal thalamus, nBOR, and midline mesencephalon receive input from small neurons, some of which are GABAergic. Moreover, these different neuronal subtypes are likely involved in different processes and behaviors related to the analysis of optic flow.

LITERATURE CITED

Arends JJA, Voogd J. 1989. Topographic aspects of the olivocerebellar system in the pigeon. Exp Brain Res Suppl 17:52–57.

Ariel M, Kogo N. 2005. Shunting inhibition in accessory optic neurons. J Neurophysiol 93:1959–1969.

Azevedo TA, Cukiert A, Britto LR. 1983. A pretectal projection upon the accessory optic nucleus in the pigeon: an anatomical and electrophysiological study. Neurosci Lett 43:13–18.

Bickford ME, Ramcharan E, Godwin DW, Erisir A, Gnadt J, Sherman SM. 2000. Neurotransmitters contained in the subcortical extraretinal inputs to the monkey lateral geniculate nucleus. J Comp Neurol 424:701–717.

Brecha N, Karten HJ, Hunt SP. 1980. Projections of the nucleus of basal optic root in the pigeon: an autoradiographic and horseradish peroxidase study. J Comp Neurol 189:615–670.

Burns S, Wallman J. 1981. Relation of single unit properties to the oculomotor function of the nucleus of the basal optic root (AOS) in chickens. Exp Brain Res 42:171–180.

Casini G, Bingman VP, Bagnoli P. 1986. Connections of the pigeons dorsomedial forebrain studied with WGA-HRP and 3H proline. J Comp Neurol 245:454–470.

Clarke PGH. 1977. Some visual and other connections to the cerebellum of the pigeon. J Comp Neurol 174:535–552.

Crowder NA, Winship IR, Wylie DRW. 2000. Topographic organization of inferior olive cells projecting to translational zones in the vestibulocerebellum of pigeons. J Comp Neurol 419:87–95.

Crowder NA, Dawson MR, Wylie DRW. 2003. Temporal frequency and velocity-like tuning in the pigeon accessory optic system. J Neurophysiol 90:1829–1841.

Cucchiaro JB, Bickford ME, Sherman SM. 1991. A GABAergic projection from the pretectum to the dorsal lateral geniculate nucleus in the cat. Neuroscience 41:213–226.

Domenici L, Waldvogel HJ, Matute C, Streit P. 1988. Distribution of GABA-like immunoreactivity in the pigeon brain. Neuroscience 25: 931–950.

Eccles JC, Llinás R, Sasaki K. 1966. The excitatory synaptic action of climbing fibers on the purkinje cells of the cerebellum. J Physiol 182: 268–296.

Erlander MG, Tillakaratne NJK, Feldblum S, Patel N, Tobin AJ. 1991. Two genes encode distinct glutamate decarboxylases. Neuron 7:91–100.

Finger TE, Karten HJ. 1978. The accessory optic system in teleosts. Brain Res 153:144–149.

Fite KV. 1985. Pretectal and accessory-optic visual nuclei of fish, amphibia and reptiles: themes and variations. Brain Behav Evol 26:71–90.

Foster TC, Castro CA, McNaughton BL. 1989. Spatial selectivity of rat hippocampal neurons: dependence on preparedness for movement. Science 244:1580–1582.

Friedman MB. 1975. Visual control of head movements during avian locomotion. Nature 255:67–69.

Frost BJ. 1978. Moving background patterns alter directionally specific responses of pigeon tectal neurons. Brain Res 151:599–603.

Gamlin PDR, Cohen DH. 1988a. Retinal projections to the pretectum in the pigeon (*Columba livia*). J Comp Neurol 269:1–17.

Gamlin PDR, Cohen DH. 1988b. Projections of the retinorecipient pretectal nuclei in the pigeon (*Columba livia*). J Comp Neurol 269:18–46.

Gibson JJ. 1954. The visual perception of object motion and subjective movement. Psychol Rev 61:304–314.

Gioanni H, Rey J, Villalobos J, Richard D, Dalbera A. 1983. Optokinetic nystagmus in the pigeon (*Columba livia*). II. Role of the pretectal nucleus of the accessory optic system. Exp Brain Res 50:237–247.

Giolli RA, Blanks RH, Torigoe Y. 1984. Pretectal and brain stem projections of the medial terminal nucleus of the accessory optic system of the rabbit and rat as studied by anterograde and retrograde neuronal tracing methods. J Comp Neurol 227:228–251.

Gottlieb MD, McKenna OC. 1986. Light and electron microscopic study of an avian pretectal nucleus, the lentiform nucleus of the mesencephalon, magnocellular division. J Comp Neurol 248:133–145.

Graf W, Simpson JI, Leonard CS. 1988. Spatial organization of visual messages of the rabbit's cerebellar flocculus. II. Complex and simple spike responses of Purkinje cells. J Neurophysiol 60:2091–2121.

Granda RH, Crossland WJ. 1989. GABA-like immunoreactivity of neurons in the chicken diencephalon and mesencephalon. J Comp Neurol 287: 455–469.

Grasse KL, Cynader MS. 1990. The accessory optic system in frontal-eyed animals. In: Leventhal A, editor. Vision and visual dysfunction, vol. IV. The neuronal basis of visual function. New York: MacMillan. p 111–139.

Graybiel AM, Berson DM. 1980. Autoradiographic evidence for a projection from the pretectal nucleus of the optic tract to the dorsal lateral geniculate complex in the cat. Brain Res 195:1–12.

Haines DE, Sowa TE. 1985. Evidence of a direct projection from the medial terminal nucleus of the accessory optic system to lobule IX of the cerebellar cortex in the tree shrew (*Tupaia glis*). Neurosci Lett 55:125–130.

Ibbotson MR, Clifford CW. 2001. Interactions between ON and OFF signals in directional motion detectors feeding the NOT of the wallaby. J Neurophysiol 86:997–1005.

Ibbotson MR, Price NS. 2001. Spatiotemporal tuning of directional neurons in mammalian and avian pretectum: a comparison of physiological properties. J Neurophysiol 86:2621–2624.

Ibbotson MR, Mark RF, Maddess TL. 1994. Spatiotemporal response properties of direction-selective neurons in the nucleus of the optic tract and the dorsal terminal nucleus of the wallaby, *Macropus eugenii*. J Neurophysiol 72:2927–2943.

Ito M, Orlov I, Yamamoto M. 1982. Topographical representation of vestibulo-ocular reflexes in rabbit cerebellar flocculus. Neuroscience 7:1657–1664.

Karten HJ, Hodos W. 1967. A stereotaxic atlas of the brain of the pigeon (*Columba livia*). Baltimore: Johns Hopkins Press.

Karten HJ, Shimizu T. 1989. The origins of neocortex: connections and lamination as distinct events in evolution. J Cogn Neurosci 1:290–301.

Karten HJ, Hodos W, Nauta WJ, Revzin AM. 1973. Neural connections of the "visual Wulst" of the avian telencephalon. Experimental studies in the pigeon (*Columba livia)* and owl (*Speotyto cunicularia).* J Comp Neurol 150:253–278.

Kawasaki T, Sato Y. 1980. Afferent projection from the dorsal nucleus of the raphe to the flocculus in cats. Brain Res 197:496–502.

Kenigfest NB, Belekhova MG, Reperant J, Rio JP, Vesselkin NP, Ward R. 2000. Pretectal connections in turtles with special reference to the visual thalamic centers: a hodological and gamma-aminobutyric acid-immunohistochemical study. J Comp Neurol 426:31–50.

Kenigfest N, Rio JP, Belekhova M, Reperant J, Vesselkin N, Ward R. 2004. Pretectal and tectal afferents to the dorsal lateral geniculate nucleus of the turtle: an electron microscopic axon tracing and gamma-aminobutyric acid immunocytochemical study. J Comp Neurol 475: 107–127.

Lau KL, Glover RG, Linkenhoker B, Wylie DR. 1998. Topographical organization of inferior olive cells projecting to translation and rotation zones in the vestibulocerebellum of pigeons. Neuroscience 85:605–614.

Leonard CS, Simpson JI, Graf W. 1988. Spatial organization of visual messages of the rabbit's cerebellar flocculus. I. Typology of inferior olive neurons of the dorsal cap of Kooy. J Neurophysiol 60:2073–2090.

Li Z, Fite KV. 1998. Distribution of GABA-like immunoreactive neurons and fibers in the central visual nuclei and retina of frog, *Rana pipiens.* Vis Neurosci 15:995–1006.

Lisberger SG, Miles FA, Zee DS. 1984. Signals used to compute errors in the monkey vestibulo-ocular reflex: possible role of the flocculus. J Neurophysiol 52:1140–1153.

McKenna O, Wallman J. 1981. Identification of avian brain regions responsive to retinal slip using 2-deoxyglucose. Brain Res 210:455–460.

McKenna O, Wallman J. 1985a. Accessory optic system and pretectum of birds: comparisons with those of other vertebrates. Brain Behav Evol 26:91–116.

McKenna O, Wallman J. 1985b. Functional postnatal changes in avian brain regions responsive to retinal slip: a 2-deoxy-D-glucose study. J Neurosci 5:330–342.

McNaughton N, Logan B, Panickar KS, Kirk IJ, Pan WX, Brown NT, Heenan A. 1995. Contribution of synapses in the medial supramammillary nucleus to the frequency of hippocampal theta rhythm in freely moving rats. Hippocampus 5:534–545.

McNaughton BL, Barnes CA, Gerrard JL, Gothard K, Jung MW, Knierim JJ, Kudrimoti H, Qin Y, Skaggs WE, Suster M, Weaver KL. 1996. Deciphering the hippocampal polyglot: the hippocampus as a path integration system. J Exp Biol 199:173–185.

Montgomery N, Fite KV, Bengston L. 1981. The accessory optic system of *Rana pipiens:* neuroanatomical connections and intrinsic organization. J Comp Neurol 203:595–612.

Morgan B, Frost BJ. 1981. Visual response properties of neurons in the nucleus of the basal optic root of pigeons. Exp Brain Res 42:184–188.

Muller RU, Ranck JB Jr, Taube JS. 1996. Head direction cells: properties and functional significance. Curr Opin Neurobiol 6:196–206.

Nagao S. 1983. Effects of vestibulo-cerebellar lesions upon dynamic characteristics and adaptation of vestibulo-ocular and optokinetic responses in pigmented rabbits. Exp Brain Res 53:36–46.

Nogueira MI, Britto LRG. 1991. Extraretinal modulation of accessory optic units in the pigeon. Braz J Med Biol Res 24:623–631.

Reiner A, Karten HJ. 1978. A bisynaptic retinocerebellar pathway in the turtle. Brain Res 150:163–169.

Robinson DA. 1976. Adaptive gain control of vestibuloocular reflex by the cerebellum. J Neurophysiol 39:954–969.

Rodriguez-Contreras A, Liu X, DeBello WM. 2005. Axodendritic contacts onto calcium/calmodulin-dependent protein kinase type II-expressing neurons in the barn owl auditory space map. J Neurosci 25:5611–5622.

Sharp PE, Blair HT, Etkin D, Tzanetos DB. 1995. Influences of vestibular and visual motion information on the spatial firing patterns of hippocampal place cells. J Neurosci 15:173–189.

Simpson JI. 1984. The accessory optic system. Annu Rev Neurosci 7:13–41.

Simpson JI, Graf W, Leonard C. 1981. The coordinate system of visual climbing fibers to the flocculus. In: Fuchs AF, Becker KA, editors. Progress in oculomotor research. Amsterdam: Elsevier/North Holland. p 475–485.

Simpson JI, Giolli RA, Blanks RHI. 1988. The pretectal nuclear complex and the accessory optic system. In: Büttner-Ennerver JA, editor. Neuroanatomy of the oculomotor system. Amsterdam: Elsevier. p 335–364.

Tang ZX, Wang SR. 2002. Intracellular recording and staining of neurons in the pigeon nucleus lentiformis mesencephali. Brain Behav Evol 60:52–58.

Theiss MPH, Hellmann B, Güntürkün O. 2003. The architecture of an inhibitory sidepath within the avian tectofugal system. Neuroreport 14:879–882.

van der Steen J, Simpson JI, Tan J. 1994. Functional and anatomical organization of three-dimensional eye movements in rabbit cerebellar flocculus. J Neurophysiol 72:31–46.

van der Want JJ, Nunes Cardozo JJ, van der Togt C. 1992. GABAergic neurons and circuits in the pretectal nuclei and the accessory optic system of mammals. Prog Brain Res 90:283–305.

Veenman CL, Reiner A, Honig MG. 1992. Biotinylated dextran amine as an anterograde tracer for single- and double-labeling studies. J Neurosci Methods 41:239–254.

Waespe W, Cohen B, Raphan T. 1983. Role of the flocculus and paraflocculus in optokinetic nystagmus and visual-vestibular interactions: effects of lesions. Exp Brain Res 50:9–33.

Wahle P, Stuphorn V, Schmidt M, Hoffmann KP. 1994. LGN-projecting neurons of the cat's pretectum express glutamic acid decarboxylase mRNA. Eur J Neurosci 6:454–460.

Weber JT. 1985. Pretectal complex and accessory optic system of primates. Brain Behav Evol 26:117–140.

Whishaw IQ, Maaswinkel H. 1998. Rats with fimbria-fornix lesions are impaired in path integration: a role for the hippocampus in "sense of direction." J Neurosci 18:3050–3058.

Whishaw IQ, McKenna JE, Maaswinkel H. 1997. Hippocampal lesions and path integration. Curr Opin Neurobiol 7:228–234.

Wild JM. 1989. Pretectal and tectal projections to the homologue of the dorsal lateral geniculate nucleus in the pigeon: an anterograde and retrograde tracing study with cholera toxin conjugated to horseradish peroxidase. Brain Res 479:130–137.

Wild JM. 1993. Descending projections of the songbird nucleus robustus archistrialis. J Comp Neurol 338:225–241.

Wilson MA, McNaughton BL. 1993. Dynamics of the hippocampal ensemble code for space. Science 261:1055–1058.

Winfield JA, Hendrickson A, Kimm J. 1978. Anatomical evidence that the medial terminal nucleus of the accessory optic tract in mammals provides a visual mossy fiber input to the flocculus. Brain Res 151:175–182.

Winship IR, Wylie DRW. 2001. Responses of neurons in the medial column of the inferior olive in pigeons to translational and rotational optic flowfields. Exp Brain Res 141:63–78.

Winship IR, Hurd PL, Wylie DRW. 2005. Spatio-temporal tuning of optic flow inputs to the vestibulocerebellum in pigeons: differences between mossy and climbing fiber pathways. J Neurophysiol 93:266–277.

Winterson BJ, Brauth SE. 1985. Direction-selective single units in the nucleus lentiformis mesencephali of the pigeon (*Columba livia).* Exp Brain Res 60:215–226.

Wolf-Oberhollenzer F, Kirschfeld K. 1994. Motion sensitivity in the nucleus of the basal optic root of the pigeon. J Neurophysiol 71:1559–1573.

Wylie DRW. 2001. Projections from the nucleus of the basal optic root and nucleus lentiformis mesencephali to the inferior olive in pigeons (*Columba livia).* J Comp Neurol 429:502–513.

Wylie DRW, Crowder NA. 2000. Spatiotemporal properties of fast and slow neurons in the pretectal nucleus lentiformis mesencephali in pigeons. J Neurophysiol 84:2529–2540.

Wylie DR, Frost BJ. 1990. Visual response properties of neurons in the nucleus of the basal optic root of the pigeon: a quantitative analysis. Exp Brain Res 82:327–336.

Wylie DR, Frost BJ. 1991. Purkinje cells in the vestibulocerebellum of the pigeon respond best to either rotational or translational visual flow. Exp Brain Res 86:229–232.

Wylie DR, Frost BJ. 1993. Responses of pigeon vestibulocerebellar neurons to optokinetic stimulation. II. The 3-dimensional reference frame of rotation neurons in the flocculus. J Neurophysiol 70:2647–2659.

Wylie DR, Frost BJ. 1996. The pigeon optokinetic system: visual input in extraocular muscle coordinates. Vis Neurosci 13:945–953.

Wylie DR, Frost BJ. 1999a. Responses of neurons in the nucleus of the basal optic root to translational and rotational flowfields. J Neurophysiol 81:267–276.

Wylie DR, Frost BJ. 1999b. Complex spike activity of Purkinje cells in the ventral uvula and nodulus of pigeons in response to translational optic flowfields. J Neurophysiol 81:256–266.

Wylie DR, Kripalani T, Frost BJ. 1993. Responses of pigeon vestibulocerebellar neurons to optokinetic stimulation. I. Functional organization of neurons discriminating between translational and rotational visual flow. J Neurophysiol 70:2632–2646.

Wylie DR, Linkenhoker B, Lau KL. 1997. Projections of the nucleus of the basal optic root in pigeons (*Columba livia)* revealed with biotinylated dextran amine. J Comp Neurol 384:517–536.

Wylie DRW, Bischof, WF, Frost BJ. 1998. Common reference frame for neural coding of translational and rotational optic flow. Nature 392: 278–282.

Wylie DRW, Glover RG, Aitchison JD. 1999a. Optic flow input to the hippocampal formation from the accessory optic system. J Neurosci 19:5514–5527.

Wylie DRW, Winship IR, Glover RG. 1999b. Projections from the medial column of the inferior olive to different classes of rotation-sensitive Purkinje cells in the flocculus of pigeons. Neurosci Lett 268:97–100.

Zanker JM, Srinivasan MV, Egelhaaf M. 1999. Speed tuning in elementary motion detectors of the correlation type. Biol Cybern 80:109–116.

Zayats N, Eyre MD, Nemeh A, Tombol T. 2003. The intrinsic organization of the nucleus lentiformis mesencephali magnocellularis: a light- and electron-microscopic examination. Cells Tissues Organs 174:194–207.

Zee DS, Yamazaki A, Butler PH, Gucer G. 1981. Effects of ablation of flocculus and paraflocculus of eye movements in primate. J Neurophysiol 46:878–899.

Zhu JJ, Lo FS. 1996. Time course of inhibition induced by a putative saccadic suppression circuit in the dorsal lateral geniculate nucleus of the rabbit. Brain Res Bull 41:281–291